Empirical Design of an On and Off Type Solenoid Actuator For Valve Operation

Baek-Ju Sung*, Eun-Woong Lee and Hyoung-Eui Kim***

Abstract - Modern users demand that the on and off type solenoid actuator should be smaller, lighter in weight, lower in consumption power, and higher in response time. The complete design satisfying such requirements can be achieved when electromagnetic theories and empirical knowledge are combined. This paper presents various types of empirical coefficients essentially needed for optimal design of a solenoid actuator. The values of these empirical coefficients are obtained through extensive experiments over a great length of time for various kinds of solenoid actuators. We have developed a design program that is composed by combination of governing equations and empirical coefficients, and have also manufactured a prototype solenoid actuator based on the final results of the design program. The propriety of the design program and empirical coefficients have been proven by experiments.

Keywords: Attraction Force, Solenoid Actuator, Space Factor, Plunger, Stationary Core

1. Introduction

The solenoid actuator is a very economical motion converter due to its simple structure. For optimal design, theoretical and empirical knowledge are simultaneously needed. Theoretical knowledge governs the operational characteristics of the solenoid actuator, and empirical knowledge compensates for the theoretical limitation obtained from the designer's design and manufacturing experiences for various kinds of solenoid actuators [1].

In particular, empirical knowledge is more essential than theoretical knowledge for determination of the plunger shape and value of the space factor because the varieties of plunger shape are very versatile and the space factor has a subjective property. As such, they cannot be determined solely by calculation or simulation. When designer's accumulated experiences and expertise are added to these, the most proper shape and value of them can then be obtained. Plunger shape affects the major characteristics of the solenoid actuator such as distribution of magnetic flux density, attraction force, and consumption power. Furthermore, the value of the space factor affects the heat dissipation and size of coil.

In this study, we derived the governing equations that represent the operating principle of the on and off type solenoid actuator for valve operation, and developed a solenoid design program composed by a combination of governing equations and empirical coefficients. As well, we manufactured a prototype of a solenoid actuator based on final results of the design program, and proved the propriety of the design program and empirical coefficients by experiments.

* Dept. of Industrial Technology, Korea Institute of machinery & Materials. (sbj682@kimm.re.kr)
** Dept. of Electrical Engineering, Chungnam National University. (ewlee@cnu.ac.kr)
Received May 9, 2003 ; Accepted April 27 2004

2. Governing Equations and Design Parameters

2.1 Structure of On and Off Type Solenoid Actuator

Fig. 1 represents the structure of an on and off type solenoid actuator. It is composed of an excitation coil, yoke for flux path, plunger for creation of mechanical stroke, stationary for attraction of the plunger, adapter for connection into mechanical apparatus, and return spring for returning of the plunger [2].

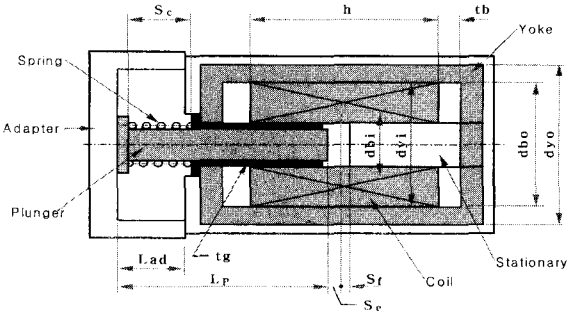

Fig. 1 Schematic of solenoid actuator

2.2 Electromagnetic Equations

Dynamic characteristics of on and off type solenoid actuators have relation to the solenoid actuator size and valve acting fluid. So, we induced the useful electromagnetic equations taking these into account. In real design, these equations can realize the desired actuator size withstanding the same attraction force by selection of proper parameter values.

Fig. 2 represents the electrical equivalent circuit of a solenoid actuator. It can only be simplified by equivalent resistance R_t in the steady state neglecting the leakage flux in the magnetic flux path, which is composed of plunger, stationary, and yoke. The relations are given to voltage equation (1) and (2) [3].

$$V = L\frac{di}{dt} + iR \tag{1}$$

$$V = iR_t \tag{2}$$

Where, L: Coil inductance, i: Current, V: Supply voltage, R: Coil resistance, R_t : Equivalent resistance of coil

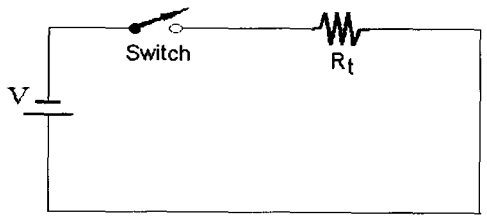

Fig. 2 Electrical equivalent circuit at steady state

2.3 Spring Force

dN is the nozzle diameter of the adapter, which offers a fluid path and is blocked by the plunger before coil excitation, P_s is supply pressure, and F_{sn} is the fluid force acting on nozzle. Then, their relation is given in equation (3).

$$F_{sn} = \frac{\pi \cdot dN^2}{4} \cdot P_s \tag{3}$$

Initial spring force F_{snc} of equation (4) should be larger than fluid acting force F_{sn}. The response time should be increased according to the increase of spring force and consumption power. As such, this characteristic has to be considered in actual design [4].

$$F_{snc} = C_l \cdot F_{sn} \tag{4}$$

Where, C_l is compensation coefficient of the initial spring force and is greater than 1.

The magnetic force F_{min} is needed for attraction of the plunger at the compressed state. L_{ad} of Fig. 1, and maximum spring force F_0 are given to equations (5) and (6), respectively.

$$F_{\min} = C_f \cdot F_{snc} \tag{5}$$

$$F_o = C_s \cdot F_{\min} \tag{6}$$

Where, C_f is compensation coefficient of magnetic force, and C_s is spring force. They should be determined by designer's experience with consideration of design limitation factors such as consumption power and rising temperature of coil [3, 4].

The final spring constant Ks is shown as equation (7) from equations (4) and (6).

$$K_s = \frac{F_0 - F_{snc}}{S_e} \tag{7}$$

Where, S_e is plunger stroke and is represented as equation (8).

$$S_e = C_{fs} \cdot dN \tag{8}$$

Where, C_{fs} is empirical value, which represents the ratio of stroke and nozzle diameter. This is related to transmission efficiency of spray pressure into the valve body [4].

2.4 Attraction Force

Acting force F and theoretical magnetic motive force U_m are shown in equations (9) and (10), respectively. Where, B is magnetic flux density, S_m is magnetic pole area, μ_0 is permeability in the air, and d is distance between magnetic poles [1, 5].

$$F = \frac{B^2 \cdot S_m}{2\mu_0} \tag{9}$$

$$B = \mu_0 \frac{U_m}{d} \tag{10}$$

Equation (11) is obtained from equations (9) and (10), and also, the design coefficient K_f is obtained from equation (12).

$$F = \frac{K_f}{d^2} \tag{11}$$

$$K_f = \frac{\mu_0 \cdot S_m \cdot U_m{}^2}{2} \tag{12}$$

When the length of fixed air gap is S_f in Fig. 1, the maximum distance d between magnetic poles is given to equation (13) that is represented by the sum of fixed air gap S_f and plunger stroke S_e. So, the maximum attraction force F_{max} and minimum attraction force F_{min} become equations (14) and (15), respectively.

$$d = S_f + S_e \tag{13}$$

$$F_{\max} = \frac{K_f}{S_f{}^2} \tag{14}$$

$$F_{\min} = \frac{K_f}{d^2} \tag{15}$$

From equations (14) and (15), the relation between maximum attraction force and minimum attraction force become equation (16).

$$F_{\max} = (\frac{d}{S_f})^2 \cdot F_{\min} \tag{16}$$

Magnetic flux density of equation (10) is equal to equation (17) by substitution of equations (9) and (15) to equation (16).

$$B = 2 \cdot \frac{\sqrt{2 \cdot \mu_0 \cdot F_{\min}}}{dl \cdot \sqrt{\pi}} \tag{17}$$

And, from equations (10) and (13), the actual magnetic motive force U, needed by the solenoid actuator, is obtained by equation (18).

$$U = \frac{C_m \cdot B \cdot d}{\mu_0} \tag{18}$$

Where, C_m is an empirical compensation coefficient for magnetic motive force[1][6]. It is needed for compensating the loss portion of magnetic force in the actual magnetic circuit.

2.5 Temperature Rising and Bobbin Length

Heat dissipation coefficient λ is the amount of heat energy radiated from the coil surface. We used the values of Fig. 3 as the coefficients, which are the experimental results of Professor Roters [1].

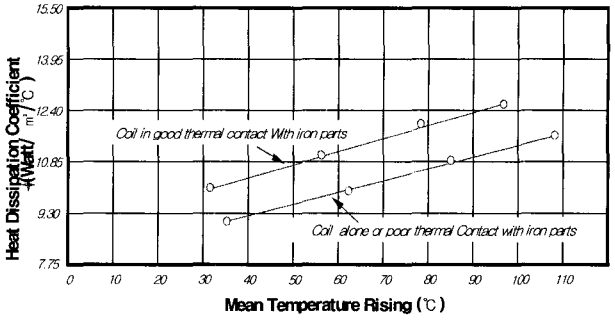

Fig. 3 Heat dissipation coefficient according to rising temperature

Coil resistance R and current I passing through it produce the rising temperature represented as T_f in equation (19). By substituting equations (20) and (21) into equation (19), we can make the constructive equation of final temperature rising as equation (22).

$$T_f = \frac{W}{\lambda \cdot S_c} = \frac{I^2 \cdot R}{\lambda \cdot S_c} \tag{19}$$

$$R = \rho \cdot \frac{(l_m \cdot N^2)}{h \cdot w \cdot X_i} \tag{20}$$

$$X_i = \frac{\pi}{4}(\frac{d_s}{d_0})^2 \tag{21}$$

$$T_f = \frac{q \cdot \rho}{2 \cdot \lambda \cdot X_i \cdot w} \cdot (\frac{N \cdot W}{h \cdot V})^2 \tag{22}$$

Where, W: consumption power, S_c: initial compressed length of spring, ρ : relative resistance, l_m: coil mean length per single turn, N: total turn numbers, h: coil height, w : coil layer thickness, q: duty ratio, I_h: current after temperature rising, d_s: diameter of bare wire, d_0: diameter of insulated coil, and V: supply voltage

Bobbin length (coil height) used in equation (22) is calculated by equation (23).

$$h = \sqrt[3]{\frac{q \cdot \beta \cdot \rho \cdot U^2}{2 \cdot \lambda \cdot X_i \cdot T_f}} \tag{23}$$

Where, β is the ratio of bobbin height h and coil layer thickness w. That is, β is equal to $\frac{h}{w}$ referring to Fig. 4, which is shown in the detailed drawing of the bobbin and yoke in Fig. 1 [4].

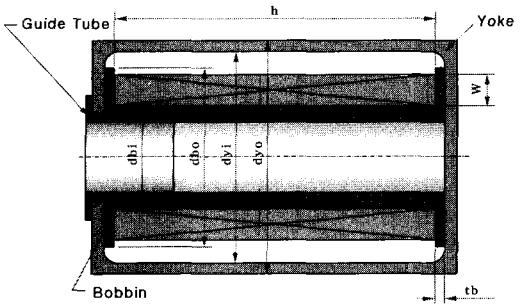

Fig. 4 Bobbin and yoke

And also, Guide tube thickness t_g, bobbin thickness t_b, coil layer thickness w, and plunger diameter dl can be found by referring to Fig. 4. So, bobbin inner diameter d_{bi}, bobbin outer diameter d_{bo}, yoke inner length d_{yi}, and yoke outer length d_{yo} are represented as equations (24) through (27), respectively.

$$d_{bi} = dl + 2(t_g + t_b) \tag{24}$$

$$d_{bo} = d_{bi} + 2w \tag{25}$$

$$d_{yi} = d_{bo} + C_g \tag{26}$$

$$d_{yo} = \sqrt{D_{yi}^{\,2} + C_p \cdot dl^2} \tag{27}$$

The empirical constant C_g in equation (26) is the length margin for smooth heat dissipation of the coil, and the empirical constant C_p in equation (27) is the length margin for smooth passing of magnetic flux.

2.6 Turn Numbers and Consumption Power of Coil

Coil mean length l_m turn is represented as equation (28).

$$l_m = \frac{\pi(d_{bo} + d_{bi})}{2} \tag{28}$$

And, the relation between voltage V and current I becomes equation (29) by using the relative resistance ρ of the copper wire.

$$V = 4 \cdot \rho\left(\frac{l_m \cdot N}{\pi \cdot d_s^2}\right) \cdot I \tag{29}$$

Diameter of bare wire, d_s is induced to equation (30) from equation (29).

$$d_s = \sqrt{\frac{2 \cdot \rho \cdot (d_{bi} + d_{bo}) \cdot U}{V}} \tag{30}$$

If it is assumed that insulated wire diameter is d_0 and the winding loss of a winding layer is 1 turn, the total turn number to be winded n_c in shaft direction given in equation (31). And, the total layer number m_c of coil in the radial direction is given by equation (32).

$$n_c = \left(\frac{h}{d_o}\right) - 1 \tag{31}$$

$$m_c = \frac{w}{d_0} \tag{32}$$

Therefore, the total turn number N to be winded on the bobbin can be given by equation (33).

$$N = n_c \cdot m_c \tag{33}$$

By combining equations (29) and (30), the equivalent resistance R_t in Fig. 2, which represents the total resistance of coil, is obtained by equation (34).

$$R_t = \frac{2 \cdot \rho \cdot (d_{bo} + d_{bi}) \cdot N}{d_s^{\,2}} \tag{34}$$

If R_t is determined, the equations of coil current I and consumption power W are determined by equations (35) and (36), respectively.

$$I = \frac{V}{R_t} \tag{35}$$

$$W = V \cdot I \tag{36}$$

2.7 Response Characteristics

The solenoid actuator can be regarded as a spring-mass system such as in Fig. 5 because it has a return spring. The plunger displacement after supplying the input voltage is equivalent to the displacement of mass m_p [7, 8].

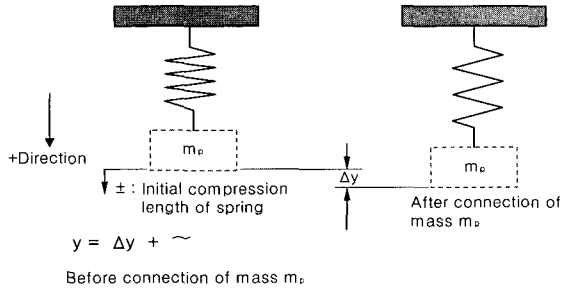

Fig. 5 The mechanical equivalent circuit of the solenoid actuator

The mass m_p of Fig. 5 is represented by equation (37), where ρ_p is material density and length L_p of the plunger.

$$m_p = \frac{dl^2 \cdot \pi \cdot L_p \cdot \rho_p}{4} \tag{37}$$

The state equation for y-direction is equation (38), and x-directional equation is equation (39). We assumed that there is no friction force in these equations because we equipped an extra guide tube at the plunger outside in the radial direction for minimizing friction and preventing the eccentricity of the plunger [3, 9].

$$m_p \ddot{y} + k_s y = m_p g \tag{38}$$

$$m_p \ddot{x} + k_s x = 0 \tag{39}$$

Therefore, the mathematical modeling to the system in Fig. 5 becomes equation (40).

$$\ddot{x} + \omega^2 \cdot x = 0 \tag{40}$$

Actuator's operating speed ω and natural frequency f_p become equation (41) and equation (42) by solving equation (40).

$$\omega = \sqrt{\frac{K_s}{m_p}} \tag{41}$$

$$f_p = \frac{\omega}{2\pi} \tag{42}$$

2.8 Empirical Value for Unknown Coefficients

Table 1 Empirical values of unknown coefficients

Name of Coefficients	Symbols	Empirical Value
Compensation coefficient for spring initial force	C_l	1.25
Compensation coefficient for minimum attraction force	C_f	1.5~2
Compensation coefficient for maximum spring force	C_s	0.75~1.25
Ratio of stroke and nozzle diameter	C_{fs}	1~2
Fixed air gap	S_f	0.2~0.25
Compensation coefficient for magnetic motive force	C_m	1.1~1.4
Ratio of bobbin height and coil width	β	1~10
Thickness of guide tube	C_g	0.004
Margin of magnetic flux path	C_p	1.25

In the prior section, the coefficients such as C_l, C_f, C_s, C_{fs}, C_m, C_g, C_p, S_e, β are unknowns. The proper values of these unknowns can't be obtained simply by theoretical simulation. The rich experiences of the designer must be added.

In this study, we used the empirical coefficients of Table 1, which are the results of our long time experiments and manufacturing for the low consumption power type solenoid actuator under 0.5W [4].

3. Design of Prototype

3.1 Design Program

Fig. 6 shows the flow-chart of the developed design program for the low consumption power type solenoid actuator, which is programmed by visual basic software based on the governing equations and empirical coefficients in Chapter 2.

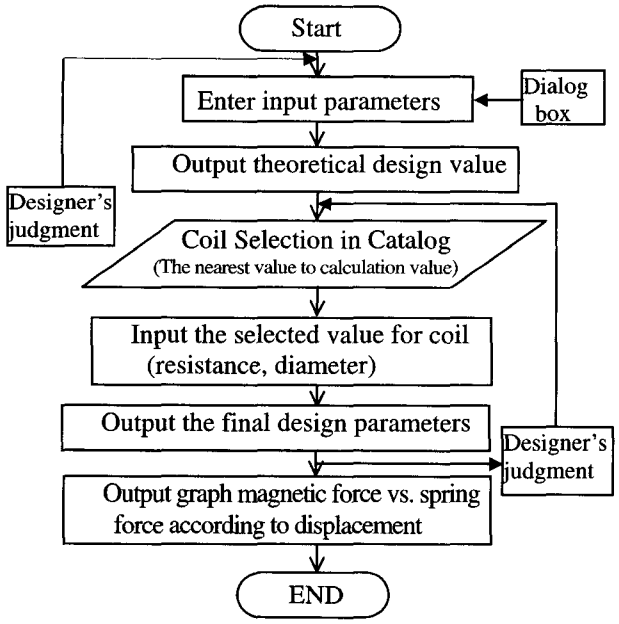

Fig. 6 Flow-chart of design program

3.2 Target Performance of Prototype

The target performance of the prototype for the pneumatic valve is as shown in Table 2.

The input parameters and their values needed for design of the prototype are introduced in Table 3. The values of parameters should be properly selected according to the target performance of the solenoid actuator.

Table 2 Target Performance

Items	Target Performance
Usage Voltage V [V]	DC24
Usage Pressure P_s [N/m^2]	980000(≈10bar)
Consumption Power W [W]	0.5
Operating Frequency f_p [Hz]	25
Temperature Rising T_f [℃]	80

Table 3 Input Parameters and Values

Parameters	Symbols	Input Values
Supply pressure [N/m^2]	P_s	980000
Nozzle diameter [m]	dN	0.0005
Fixed air gap [m]	S_f	0.00023
Plunger diameter [m]	dl	0.004
Temperature rising [℃]	T_f	80
Temperature rising [℃]	T_f	80
Voltage DC [V]	V	24
Plunger length [m]	L_p	0.01
Compensation value (F/F_{sn}) for F	C_f	1.1
Ratio of stroke and nozzle diameter (Se/dN)	C_{fs}	1
Ratio of max. magnetic motive force to max. spring force	C_s	1.2
Ratio of voltage variation	f_v	1
Compensation value of magnetic motive force	C_m	1.1
Coil height (h) / Coil width (w)	ß	2.86
Heat dissipation coefficient (at 80℃)	λ	10.7
Guide tube thickness [m]	t_g	0.00065
Bobbin thickness [m]	t_b	0.00155
Bare wire diameter [m]	d_s	Selection at standard coil catalog
Insulated wire diameter [m]	d_0	Selection at standard coil catalog
Coil resistance per unit length (at 20℃)	rcm	Selection at standard coil catalog
Duty ratio (=1)	q	Internal input
Permeability in free space [Wb/A.T]	μ_0	Internal input
Relative resistance of copper wire [Ω .m]	ρ	Internal input

3.3 Design Results

By input of the values in Table 3 to the design program, we can obtain the results of Table 4 as a numerical output, and also obtain the curves of Fig. 7 as a graphical output, which represent stroke versus spring force F_{sp} and attraction forces, F_x, F_s, and F_h.

Table 4 Output Parameters

Parameters	Symbols	Output Values
Magnetic flux density [T]	B	0.2057497
Plunger diameter [m]	dl	0.004
Plunger sectional area [m^2]	S_m	1.256636E-05
Magnetic motive force [A.T]	U	97.40054
Coil height [m]	H	1.018737E-02
Coil width [m]	w	3.562019E-03
Bobbin inner diameter [m]	d_{bi}	8.040000E-03
Bobbin outer diameter [m]	d_{bo}	1.552404E-02
Coil diameter [m]	d_s	7.71369E-05
Turn number of coil [Turn]	N	4342.991
Coil resistance [Ω]	R_t	962.6605
Current [A]	I	2.242758E-02
Consumption power [W]	W	0.538262
Temperature rising [℃]	T_f	65.69974
Operating frequency [Hz]	f_p	26.38521

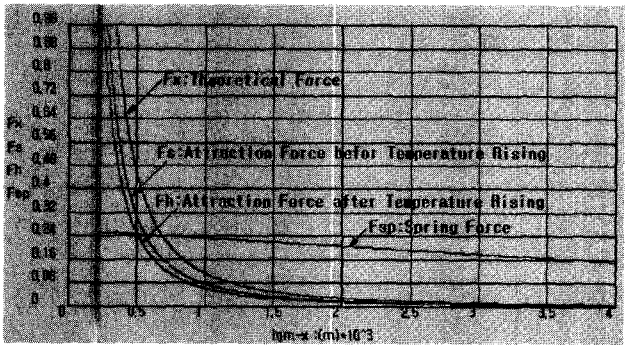

Fig. 7 Attraction forces and spring force according to stroke

4. Manufacturing of Prototype and Analysis of Experimental Results

4.1 Manufacturing of Prototype and Experiments

The prototype actuator is made by use of the design parameters in Table 2. We used K-M series of the East-North Special Steel Co. in Japan as magnetic material that does not saturate at required magnetic flux density of 0.2[T]. Korean standard coil was used for coil winding of the solenoid actuator. Its bare wire diameter is 0.07mm, which is the nearest to the design value of 0.077mm. Experiments were performed by way of a general performance and durability tester for the pneumatic valve, which was equipped in the Reliability Evaluation Center of the Korea Institute of Machinery & Materials

4.2 Experimental Results

Fig. 8 represents a typical step response characteristic of the solenoid actuator with a 3-step period during

current build-up. It shows the increasing period from starting point "a", temporary decreasing period owing to reluctance reduction (point "b"), and increasing and settle down period at rated current (hereafter point "b"). We can predict the operating time of the solenoid actuator in this figure. That is, the time required from point "a" to "b", about 2.5ms, is the operating time needed for complete attraction of the plunger onto the stationary.

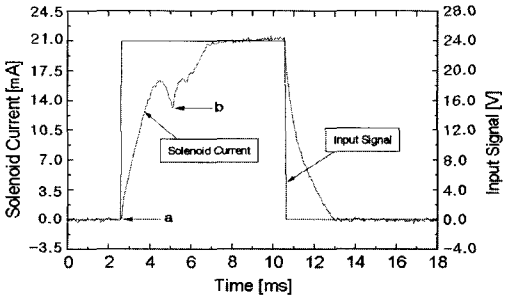

Fig. 8 Step input wave of current

Fig. 9 represents the moving trace of the plunger according to the current build-up. This is measured through an acceleration sensor that is adhered on the radial surface of the solenoid actuator for verifying the attraction point of the plunger. We know that the plunger is exactly attracted onto the stationary at the rising point of maximum amplitude of the acceleration sensor. The attraction point and required time for complete attraction are almost identical with the presented in Fig. 9.

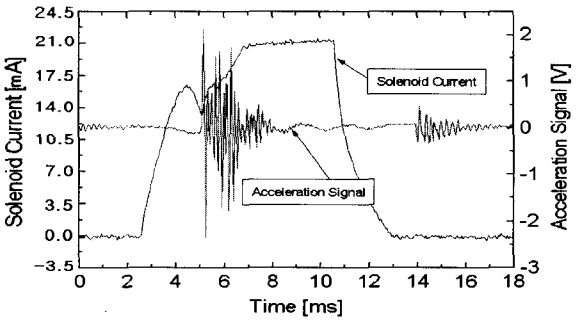

Fig. 9 Moving trace of plunger according to current build-up

Fig. 10 shows the graph of measured consumption power for the prototype solenoid actuator. From this graph, we know that the consumption power stabilizes at approximately 0.52W, and this is very similar to 0.538W, which is the output value of the design program used to design the target of 0.5W.

Fig. 11 is a measured graph of temperature variation after voltage supply. The upper value of temperature rising is about 70℃, and this signifies that the temperature rising of the coil is stabilized at under 80℃, which is the design target.

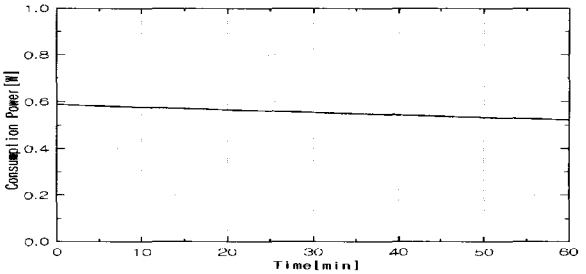

Fig. 10 Measuring result of consumption power

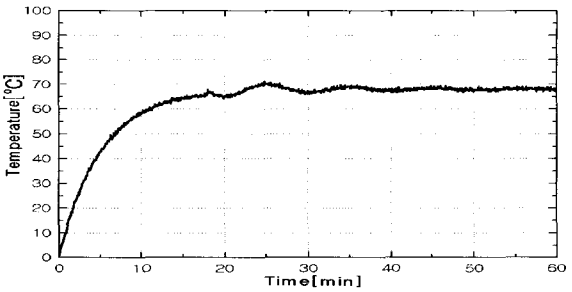

Fig. 11 Measuring result of temperature rising

Fig. 12 represents the frequency response characteristic of the prototype solenoid actuator when input frequency is 25Hz. From this graph, we know that the solenoid actuator is following up the input frequency very well. This means that the operating speed of this solenoid actuator completely satisfies the output value of the design program (26Hz) and the design target (25Hz).

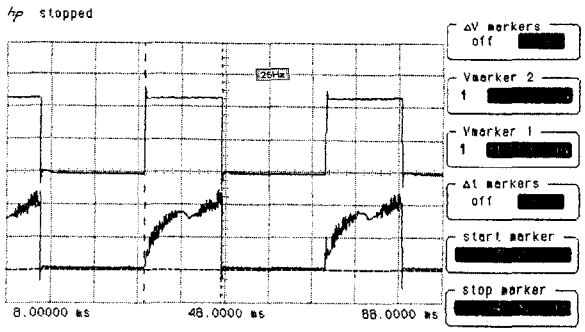

Fig. 12 Frequency response characteristics

5. Conclusions

In this paper, governing equations and unknown design coefficients are derived and a design program for a solenoid actuator is composed. We also manufactured the prototype solenoid actuator by use of the results of the design program and obtained the following experimental results.

1) We verified the validity of empirical coefficient values for the prototype solenoid actuator because the prediction result of attraction time in Fig. 8 agreed with

the step input wave of the current wave in Fig. 9, which is the result of real measurement using an acceleration sensor.

2) The accuracy of the examined theories and design program are proved by consideration of the following. The consumption power of prototype solenoid actuator approaches the target value of 0.5W as 0.52W, temperature rising is stabilized at under 80℃ as 70℃. Furthermore, the operating frequency also approaches the target value of 25Hz as 26Hz.

3) The performance of the prototype solenoid actuator was satisfactory from the viewpoint of the valve operation. We will introduce more detailed experimental results in the next paper including the results of reliability and environmental testing.

References

[1] C. Roters, "Electro magnetic device", John Wiley & Sons, Inc, 1970

[2] B. J. Sung, E. W. Lee, H. E. Kim, "Development of design Program for on and off type solenoid actuator", Proceedings of the KIEE Summer Annual Conference 2002(B), pp929~931, 2002. 7. 10

[3] B. S. Kang, S. N. Yun, B. J. Sung, H. E. Kim, "Study on characteristics of high-speed magnet for PWM control", Annual Papers of Korea Institute of Machinery & Materials, Volume 27, pp141~pp151, 1997.12

[4] Hydraulic and Pneumatic Lab. of KIMM, "Development of low consumption power type solenoid valve", KIMM-CSI Annual Report, 2001. 12

[5] H. Hayt, "Engineering electromagnetics", Mc. Grawhill, 1986

[6] S. N. Yun, B. J. Sung, "The study on characteristics for flow controlled force feedback type servo valve ", Proceedings of the KSME Fall Annual Conference, 1999. 11. 6

[7] K. Ogata, "System dynamics", Prentice Hall, 1998. 1

[8] T. Kajima, "Dynamic model of the plunger type solenoid at deenergizing state", IEEE Transactions on Magnetics, Vol.31, No.3, pp2315~2323, May 1995

[9] T. Kajima, S. Satoh, R. Sagawa, "Development of high-speed solenoid valve", JIEE(Part C) Volume 60, No. 576, pp254~261, 1994. 8

Baek-Ju Sung

He received his B.S. and M.S. degrees in Electrical Engineering from Busan National University in 1990 and 1992, respectively. He currently works at the Korea Institute of Machinery & Materials. He is working toward a Ph. D. degree at Chungnam National University.

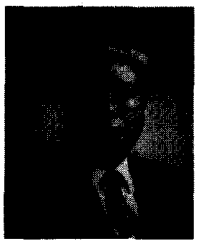

Eun-Woong Lee

He received his B.S., M.S., and Ph. D. degrees in Electrical Engineering from Hanyang University, Korea, in 1971, 1974, and 1983, respectively. From Mar. to Dec. 1976, he was a Faculty of the Daejon Junior Technical College. Since 1976, he has been a Professor in the Department of Electrical Engineering, Chungnam National University, Daejon, Korea. From 1982 to 1983 and 1985 to 1986, he was a Visiting Professor in the Department of Electrical Engineering, McGill University, Montreal, Canada. From 1999 to 2002, he was Vice President and Acting President of "The Korean Federations of Teachers Associations". Now he serves as President of the "Korean Institute of Electrical Engineering (KIEE)", and Vice President of the "Korea Electric Engineers Association" and the "Korea Electric Association". His interests are in the areas of electrical machines, special purpose motors, and power quality. He has been a Senior Member of IEEE, and is a lifetime member of KIEE.

Hyoung-Eui Kim

He received his B.S. degree in Mechanical Engineering from Aju University, Korea, in 1978, and his M.S. degree in Hydraulic Control from K.A.I.S.T, Korea, in 1980. He also received his Expert M.S. and Ph.D. degrees in Automatism and Pneumatic Control from I.S.M.C.M, France, in 1982 and 1985, respectively. In 1990, he was the recipient of the Minister prize from the Korean Ministry of Science & Technology, and recipient of the Minister prize from the Korean Ministry of Commerce, Industry and Energy in 2004. He is now a Director of the Reliability Center in the Field of Machinery Elements at the Korea Institute of Machinery & Materials. His research interest is in the area of design and assessment of hydraulic & pneumatic elements.